Case Studies in Construction Materials 21 (2024) e03527

Contents lists available at ScienceDirect

Case Studies in Construction Materials

journal homepage: www.elsevier.com/locate/cscm

Experimental investigation on durability of prefabricated rollable asphalt: Creep and fatigue performance evaluation

Mahdi Shojaei, Hajar Share Isfahani *, Sayyed Mahdi Abtahi

Researcher, Dept. of Civil Engineering, Isfahan University of Technology, Isfahan 84156-83111, the Islamic Republic of Iran

ARTICLE INFO

Keywords:
Rollpave
Prefabricated asphalt
Asphalt mat
Modular pavement
Rollable asphalt

ABSTRACT

Rollpave, a thin prefabricated rollable asphalt layer produced in a factory and rolled on a reel for laying on the existing surface, has attracted attention in the pavement industry due to its rapid treatment capabilities. However, the long-term durability of Rollpave needs further evaluation before considering widespread use. This study aims to assess the durability of Rollpave by evaluating the fatigue and creep performance of its modified bitumen and asphalt mixture. The results highlight that the creep stiffness of modified bitumen at −12°C is half of the corresponding value of virgin bitumen, and lowering the temperature to −18°C increases its creep stiffness to 78.44 MPa. At the same time, it is still 20 MPa less than virgin bitumen. Besides, it is showed the fatigue life of modified bitumen is 23 times greater than the corresponding value of virgin bitumen at 20°C and strain levels of 5 %, and modified bitumen has better stress relaxation ability leading to damage endurance. Additionally, it is observed that the flexural stiffness of the Rollpave mixture drops by only 23 % after 600,000 cycles under 400 με repeated loading. Furthermore, it is indicated that although the creep performance of Rollpave is sensitive to stress and temperature, it has a noticeable recovery ability and rutting resistance, with the average value of non-recoverable creep compliance and percent recovery at stress level of 3.2 kPa at 64°C being 0.213 kPa^{-1} and 54 %. The asphalt dynamic creep test results of the Rollpave mixture also indicated nearly 20,000 με of cumulative permanent strain at 50°C in the 9000_{th} loading cycle.

1. Introduction

Different options of pavement treatment exist to improve functional conditions and lessen surface degradation. A thin asphalt overlay is one of the commonplace options to restore the capacity of in-service pavements [1]. However, overlaying, in general, is time-consuming and causes traffic congestion due to the transportation, distribution, and compaction process of the asphalt mixture. Therefore, Rollpave was introduced as a modern alternative to pavement maintenance technology [2-5]. Rollpave is a thin prefabricated rollable asphalt layer that reduces the road closure time required for pavement maintenance [4,6,7]. Also, a study by Tan et al. has shown that a prefabricated flexible ultrathin overlay maintained good waterproofing, skid and crack resistance, and interlayer bonding properties after a medium-scale accelerated loading test while its thickness was only about one-third of traditional overlays [8].

Having been unrolled like a carpet on the existing surface, Rollpave does not need any asphalt paver, and it can be bonded to the underlying surface using electromagnetic waves [4]. Even though this rolling and unrolling process causes small cracks on Rollpave, it

* Corresponding author.
E-mail addresses: mahdishojaee@alumni.iut.ac.ir (M. Shojaei), hajarshare@iut.ac.ir (H. Share Isfahani), mabtahi@iut.ac.ir (S.M. Abtahi).

https://doi.org/10.1016/j.cscm.2024.e03527
Received 21 February 2024; Received in revised form 27 June 2024; Accepted 13 July 2024
Available online 14 July 2024

is proven that it has an adequate self-healing performance to restore its stiffness and strength by closing the cracks [9]. Dong et al. investigated self-healing performance of Rollpave at different temperatures (-10°C, 10°C, and 30°C), damage levels, and bitumen ratio. The findings indicated that the optimal self-healing performance of the asphalt mixture occurs at 10°C. Furthermore, higher bitumen content increased the self-healing capability of Rollpave [9].

Another advantage of Rollpave technology is that it can considerably improve the construction speed and quality of asphalt pavement [10-12]. Also, it has been shown that the application of Rollpave is acceptable for paving motorways, urban roads, bridge decks, and parking decks [4]. In addition, using Rollpave can be a perfect approach for maintaining road sections in a period with temperatures under the freezing point, when laying hot mix asphalt is impossible [4]. Another study evaluated the effect of basalt fiber content on the performance of Rollpave. The results show that with the increase of basalt fiber content by 0, 0.1 %, 0.3 %, and 0.5 %, the rutting test dynamic stability, low temperature bending failure strain and water immersion Marshall residual stability of asphalt mixture increase first and then decrease. However, normal temperature bending failure strain gradually increased [13].

Moreover, another investigation revealed the beneficial applications of Rollpave and proposed a prefabricated flexible conductive composite overlay for active de-icing and snow melting. This overlay serves as a temperature-adjusting layer that effectively overcomes the impact of ice and snow on pavement structures and road safety. The results indicate two significant advantages of this overlay including higher electrothermal conversion efficiency and excellent flexibility. The electrothermal conversion efficiency may reach 29.10 % and 66.05 % for melting ice and frost, respectively. Additionally, the overlay has the potential to relieve distress caused by ice and snow, particularly in critical infrastructure such as bridges, tunnel portals, and airport runways. It also meets the requirements for deformation and maintaining stability after repeated loading. Furthermore, it exhibits favorable skid resistance performance, meeting requirements for road surface friction [14].

Tan et al. presented a comprehensive and systematic review of prefabricated technology in pavement engineering. They mentioned that this technology enhances construction efficiency while mitigating the human and environmental impacts of asphalt fumes produced by traditional asphalt paving. During tunnel asphalt pavement construction, substantial amounts of asphalt fumes are generated and are difficult to eliminate, posing significant health risks to workers. In contrast, the prefabricated technology releases virtually no harmful substances during the construction process, thereby safeguarding worker health, and it is a high-efficiency, energy-saving, carbon-reducing, quality-controlled, and environmentally friendly pavement technology [15].

Despite the previous studies on Rollpave [2,9,16,17], the durability of prefabricated rollable asphalt, including fatigue and creep performance, is still one of the main concerns and needs further evaluation. In the other words, the potential proficiency of this technology to resist against fatigue and creep damages has not been assessed yet. Therefore, this study aims to assess the fatigue and creep behaviors of the asphalt mixture and the modified bitumen of Rollpave to justify its widespread application. To achieve these goals, Bending Beam Rheometer (BBR), Linear Amplitude Sweep (LAS), and Multiple Stress Creep Recovery (MSCR) tests were carried out on Rollpave Modified Bitumen (RMB). Also, four-point beam fatigue and dynamic creep tests were conducted on corresponding asphalt specimens. This paper is divided into six sections, starting with the specification of the materials used to prepare Rollpave, followed by the introduction of the mixture's design. The subsequent section provides an overview of the laboratory test methods used. The experimental results are then thoroughly examined, and the study's conclusion is finally presented.

2. Materials

The crushed aggregate used in this study was supplied by a limestone quarry in Isfahan City, Iran. Table 1 presents the physical properties of the fine and coarse aggregates, and Fig. 1 shows the gradation of utilized aggregates. Moreover, the most common and available bitumen in Iran, PG 64–22, was used as a virgin bitumen and compared with RMB.

In this study, RMB as a highly modified bitumen was particularly developed by experimental procedure. RMB consists of three components along with virgin bitumen: (1) compounding agent, (2) ductile agent, and (3) modified thermoplastic elastomer. The compounding agent is a bio-oil additive, which substitutes for 10 wt% of bitumen to disperse the particles and keep them in a colloidal state. The ductile agent, a flexible component stretching up to 5 times the original length, is used at 5 wt% of bitumen. Table 2 and Table 3 demonstrate the characteristics of the compounding agent and ductile agent, respectively. The thermoplastic elastomer modified by Ethylene Propylene Diene Monomer (EPDM), shown in Fig. 2, is used at 12 wt% of bitumen to increase its elastic properties. In this study, the combination of aforementioned components named Rollbit. Moreover, the required specifications of Rollpave bitumen and mixture were controlled with the previous results shown by Dong et al. [2].

Table 1
Physical properties of coarse and fine aggregates.

Test title		Result	Test method
Coarse Aggregates:			
Los Angeles abrasion, %		26	ASTM C131
Elongated particle, %		19	BS-812
Flattened particle, %		26	
Crushing value, %	One side	99	ASTM D5821
	Two side	96	
Fine Aggregates:			
Crushing value, %		46	ASTM C1252
Sand Equivalent, %		58	ASTM D2419

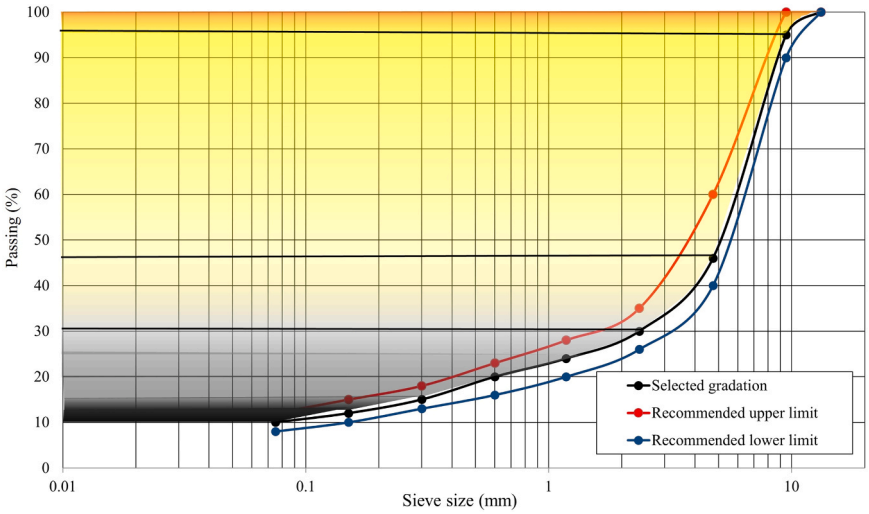

Fig. 1. The gradation curve of HMA aggregates.

Table 2
Characteristics of the compounder agent of RMB.

Property	Result
Appearance	yellow
Flashpoint (°C)	280
Freezing Point (°C)	-4
Density (g/cm^3)	0.985
Molecular weight (kg/kmol)	1000
Epoxy value	4

Table 3
Characteristics of the ductile agent of RMB.

Property	Result
Density (g/cm^3)	1.02
Break strength (MPa)	8.6
Elongation at Break (%)	410

Fig. 2. The modified thermoplastic elastomer of RMB.

In order to develop RMB in this study, the virgin bitumen was heated to 170°C in an oven to achieve the homogenous modified bitumen. Then, the above mentioned modifiers were gradually mixed with the virgin bitumen at 4000 rpm using a high-shear laboratory mixer for approximately an hour at 170°C. To better understand the characteristics of RMB, the physical properties and G* values were measured and compared with the virgin bitumen using the conventional and Dynamic Shear Rheometer (DSR) tests, and the results are shown in Table 4 and Fig. 3.

3. Mixture design and sample preparation

In this study, aggregates and RMB were preliminarily heated to nearly 170°C to mix together until reaching a uniform mixture. It is worth mentioning that the approach presented by the previous study has been implemented to obtain the optimum RMB content for Rollpave [2]. It has been documented that a minimum of 2400 times/mm for dynamic stability and a minimum of 5 mm deflection of the three-point beam bending test are Rollpave mixture design requirements [2,9]. Accordingly, 7.5 % RMB of the aggregate weight was selected as the optimum RMB content in this study. Fig. 4 shows a small laboratory sample of Rollpave which was prepared with the aforementioned mixture design and materials. This sample was rolled on a reel with a diameter of 1.1 m, and after a week unrolled on a road.

In this study, six cylindrical and two slab samples of Rollpave were prepared using the Superpave Gyratory Compactor (SGC) and slab compactor, respectively, for dynamic creep test and four-point beam fatigue test. The cylindrical samples had dimensions of 67 ±1 mm in height and a diameter of 100 mm, while each slab sample was cut into three beam samples with dimensions of 63±1 mm by 50±1 mm by 385±1 mm. All creep and fatigue specimens were compacted to the target air void of 4 % at a temperature of 140°C.

4. Experimental methods

This section summarizes the methods used to study the properties of RMB and Rollpave mixture. The BBR and MSCR tests were carried out to investigate the creep performance, and the fatigue performance was appraised through the LAS test. Regarding the asphalt mixture, four-point beam fatigue and dynamic creep tests were conducted to evaluate the Rollpave performance.

4.1. Bitumen bending beam rheometer test

It is reported that the relaxation ability is a strong indicator of bitumen durability, and it is essentially a pointer of bitumen cracking since a decrease in relaxation ability leads to stress accumulation and thus cracking [18]. Also, low temperature cracks are one of the significant distresses of pavement, depending on bitumen characteristics [19]. To measure low-temperature cracking properties of bitumen, the BBR test has been implemented according to ASTM D6373–16. In this test, the flexural creep stiffness, S(t), and m-value were measured. S(t) reflects the low-temperature cracking resistance of bitumen and the m-value represents the slope of the creep stiffness versus the time curve in a log-log scale [20]. At first, the long-term aging was simulated by the pressure aging vessel (PAV), standard ASTM D6521. Afterward, the BBR test was conducted on RMB and virgin bitumen at −12°C and −18°C.

4.2. Bitumen multiple stress creep recovery test

To characterize the creep behaviour of polymer-modified bitumen under various loading frequencies, the MSCR test was used [21]. The MSCR test includes a standard rheological test protocol whereby an aged bitumen through rolling thin-film oven test (RTFOT), standard ASTM D2872, is subjected to a creep load for 1 s at 0.1 kPa and 3.2 kPa stress levels and 9 s recovery based on AASHTO T 350. This study assessed RMB at four temperatures of 64°C, 70°C, 76°C, and 82°C and compared the results with virgin bitumen. The average percent recovery ($R_{(\tau)}$), the average non-recoverable creep compliance for each stress level ($Jnr_{(\tau)}$), and the percent difference between Jnr were computed following MSCR protocol as shown in Eqs. 1 to 3. AASHTO M332 establishes a maximum threshold on J_{nrdiff} to prevent the utilization of bitumen with high sensitivity to stress. It is noted that bitumen exceeding a J_{nrdiff} value of 75 % is considered rutting susceptible to load or temperature changes.

$$R_{0.1} = \frac{SUM[\varepsilon_r(0.1, N)]}{10}, \text{ and } R_{3.2} = \frac{SUM[\varepsilon_r(3.2, N)]}{10} \quad (1)$$

Table 4
Conventional properties of RMB.

Property	Result	
	RMB	Virgin bitumen
Penetration (1/10 mm)	63.3	67
Ductility @ 25°C (cm)	88*	125
Ductility @ 5°C (cm)	63	4
Softening point (°C)	At least 100	52.4

* Ductility apparatus could not pull it more.

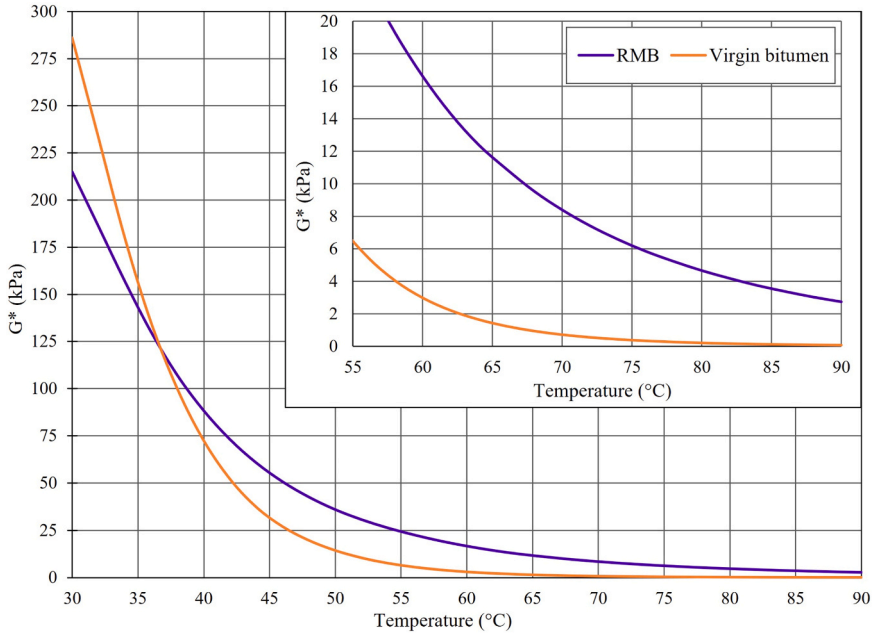

Fig. 3. G* values of RMB and virgin bitumen.

Fig. 4. Laboratory Rollpave sample.

$$J_{nr0.1} = \frac{SUM[J_{nr}(0.1, N)]}{10}, \text{ and } J_{nr3.2} = \frac{SUM[J_{nr}(3.2, N)]}{10} \tag{2}$$

$$J_{nr_{diff}} = \frac{\left(J_{nr_{3.2}} - J_{nr_{0.1}}\right) \times 100}{J_{nr_{0.1}}} \tag{3}$$

Where:

ε_r (0.1, N) and ε_r (3.2, N) are the strain recovery values for each cycle, N, at the creep stress level of 0.1 kPa and 3.2 kPa. And J_{nr} (0.1, N) and J_{nr} (3.2, N) are the non-recoverable creep compliance values for each cycle, N, at the creep stress level of 0.1 kPa and 3.2 kPa.

4.3. Bitumen linear amplitude sweep test

The LAS test was conducted according to AASHTO T101–14. This test consists of two steps performed on PAV-aged samples. In the first step, a frequency sweep applies oscillatory shear loading at a constant load of 0.1 % strain over frequencies from 0.2 Hz to 30 Hz.

Then, an amplitude sweep test is carried out at a frequency of 10 Hz while strain increases linearly from zero to 30 percent. To calculate the fatigue life of bitumen, the undamaged material property (α) was computed from frequency sweep test data as shown in Eq. 4. Afterward, a method documented by Kim et al. was used to calculate damage accumulation (D(t)) and damage accumulation at failure (D_f), as illustrated in Eqs. 5 to 7 [22]. Finally, the fatigue performance parameter, N_f, was determined using the power law expressed in Eqs. 8 to 10.

$$\alpha = \frac{1}{m} \tag{4}$$

$$D(t) \cong \sum_{i=1}^{N} \left[\pi\gamma_0^2 (C_{i-1} - C_i)\right]^{\frac{\alpha}{1+\alpha}} (t_i - t_{i-1})^{\frac{1}{1+\alpha}} \tag{5}$$

$$C(t) = \frac{|G^*|(t)}{|G^*|initial} \tag{6}$$

$$D_f = \left(\frac{C_0 - C_{at\ peak\ stress}}{C_1}\right)^{\frac{1}{C_2}} \tag{7}$$

$$A = \frac{f(D_f)^{(1+(1-C_2)\alpha)}}{(1+(1-C_2)\alpha)(\pi C_1 C_2)^{\alpha}} \tag{8}$$

$$B = 2\alpha \tag{9}$$

$$N_f = A(\gamma_{\max})^{-B} \tag{10}$$

Where:

m is the slope of the storage modulus versus loading frequency results from the frequency sweep test plotted in a logarithmic scale. And γ_0 and γ_{max} are the applied strain for a given data point and the maximum expected binder strain for a given pavement structure, percent.

C(t) is the integrity of material.

$|G^*|(t)$ and $|G^*|_{initial}$ are modulus at time and initial modulus.

t is testing time, second.

f is loading frequency (10 Hz).

C_0, C_1, C_2, A, and B are the curve-fit coefficients of the model.

The 'A' parameter directly affects the fatigue life, and the 'B' parameter represents the sensitivity of fatigue life to strain level change. Generally, bitumen with a higher 'A' value and a lower absolute 'B' value gives rise to a pavement with a longer service life.

Fig. 5. The Universal Testing Machine in this study.

This study evaluated and compared virgin bitumen and RMB fatigue performance at a temperature of 20°C. Also, the linear amplitude sweep test was conducted on RMB at 30°C to assess the temperature susceptibility of RMB's fatigue life.

4.4. Asphalt four-point beam fatigue test

One of the crucial damage which significantly poses threat to the durability of thin asphalt layers is fatigue cracking [23]. In this regard, the fatigue performance of Rollpave was evaluated at 20°C using the four-point beam fatigue test according to AASHTO T321. The samples underwent five hours inside a temperature-controlled cabinet to guarantee a balanced temperature. Then, the specimens were subjected to a strain-controlled mode of sinusoidal loading with a frequency of 10 Hz. Firstly, the stiffness and fatigue resistance of specimens were evaluated during 36,000 cycles at a constant strain of 200 με. However, since the reduction of flexural stiffness was insignificant, a new trial with 400 με was carried on for about 600,000 loading cycles on new samples. Subsequently, the average results were subjected to the Weibull Survivor Function to determine the fatigue failure life of Rollpave and corresponding fatigue damage [24,25].

4.5. Asphalt dynamic creep test

Permanent deformation is the progressive accumulation of deformation of each layer of the pavement structure under repetitive traffic loading; however, the asphalt layer has a noticeable role in its magnitude [26]. Additionally, the dynamic creep test has a very good correlation with measured deformation and gives results allowing the characterization of the mixes in terms of their long-term deformation behavior [27]. Therefore, after placing the samples in a temperature-controlled chamber for five hours to reach temperatures of 50°C and 60°C, the dynamic creep test was carried out using a Universal Testing Machine (UTM), as shown in Fig. 5, according to Australian code AS 2891.12.1. Generally, the deformation of specimens starts to increase by application of stress during the pulse width, and it climbs up to its highest point as the loading is finalized. During the rest period, a considerable portion of deformation which is known as resilient deformation disappears, and the remaining deformation is considered to be permanent deformation [26].

The loading parameters in this study consisted of a square waveshape with a stress level of 400 kPa applied for 0.5 s, followed by a rest period of 1.5 s. The test was terminated after 9000 load cycles or reaching 30,000 με. Test results were analyzed to determine the permanent deformation parameters, such as the dynamic creep curve and ultimate strain. The accumulated permanent strain was calculated by dividing the axial deformation in each cycle by the initial specimen height, and finally, creep models were derived based on Zhou's three-stage model [28].

5. Results and discussion

This section presents the results and discussion of the investigation into the properties of RMB and Rollpave mixture.

5.1. Bitumen bending beam rheometer test

By conducting the BBR test, the creep performance of PAV-aged RMB was evaluated at −12°C and −18°C. However, the creep performance of virgin bitumen was assessed only at −12°C since its low-temperature grade was −22°C. Table 5 indicates that RMB had a reduced creep stiffness and an increased m-value compared to virgin bitumen at −12°C. Furthermore, RMB met the ASTM-D6648 specifications by exhibiting a stiffness of less than 300 MPa and an m-value greater than 0.3 at both −12°C and −18°C. This performance helps mitigate thermal cracking at low temperatures.

RMB's creep stiffness at −12°C decreased by more than 50 percent compared to the virgin bitumen. The observed reduction in stress relaxation property in RMB could be attributed to the inclusion of the bio-oil additive, generally composed of aromatics, resins and saturates, in RMB which improves the stress relaxation property. Moreover, the lower modulus and stiffness of the bio-oil and ductile agent compared to the bitumen at low temperatures may explain this effect. Also, lowering the temperature to −18°C increased the RMB creep stiffness from 48.02 MPa to 78.44 MPa. Generally, a smaller creep stiffness value refers to better flexibility of bitumen, and a higher m-value indicates superior stress relaxation and crack resistance of bitumen. The ductility value at 5°C, as demonstrated in Table 4, also confirmed the improved flexibility of RMB compared to virgin bitumen.

What stands out in this table is that despite a 6-degree drop in temperature to −18°C, the RMB creep stiffness is even less than virgin bitumen creep stiffness at −12°C. This is thoroughly suitable because it increases deformability, especially at low temperatures. Moreover, this indicates that RMB has better relaxation ability and low-temperature properties than virgin bitumen. It is reported that

Table 5
Creep stiffness and m-value of PAV-aged bitumen and RMB.

Temperature	RMB		Virgin bitumen	
	m-value	S(t) (MPa)	m-value	S(t) (MPa)
-12°C	0.340	48.02	0.302	98.70
-18°C	0.300	78.44	-	-

the relaxation ability is a strong indicator of bitumen durability, and it is essentially a pointer of bitumen cracking since a decrease in relaxation ability leads to stress accumulation and thus cracking [18]. Concludingly, Rollpave can be less sensitive to cracking and has superior durability.

5.2. Bitumen multiple stress creep recovery test

After the RTFO aging process, the MSCR test was conducted on both RMB and virgin bitumen. Fig. 6 shows the average percent recovery at both stress levels versus temperature. It reveals that the incorporation of Rollbit increased $R_{0.1}$ and $R_{3.2}$ in all testing temperatures compared to the corresponding values of virgin bitumen. For instance, the $R_{0.1}$ and $R_{3.2}$ values of RMB are more than 11 and 67 times the corresponding values of virgin bitumen at 64°C. Generally, $R_{0.1}$ and $R_{3.2}$ reduced while the temperature or stress level increased; however, $R_{0.1}$ of RMB negligibly rose when the temperature increased from 64 to 70°C. This behavior is attributed to the thermoplastic elastomer network, which may not be wholly stretched at 64°C and did not function at its total capacity. Similar observations on SBS-modified bitumen were also reported by another study [18].

It can be seen in Fig. 6 that the average percent recovery of RMB at 64°C declined by 33.9 units with an increase in the stress level to 3.2 kPa. In contrast, the corresponding value of the virgin bitumen is just seven units. Furthermore, the results illustrate that the average percent recovery of RMB declines substantially at both stress levels compared to virgin bitumen. This indicates that RMB is comparatively more sensitive to stress and temperature changes, though RMB significantly resists permanent deformation at elevated temperatures. To be more specific, $R_{3.2}$ of RMB at 82°C was four times the corresponding value of virgin bitumen at 64°C. The negative value of $R_{3.2}$ of the RTFO-aged virgin bitumen at 70°C means an inability to recover the strains; in other words, it signifies that the virgin bitumen reached a flow phase.

Table 6 consists of the values of $J_{nr0.1}$, $J_{nr3.2}$, and J_{nrdiff}. According to the data, the J_{nr} values of RMB at both stress levels decreased outstandingly, indicating enhanced rutting resistance. For example, Rollbit modification decreased $J_{nr0.1}$ and $J_{nr3.2}$ of virgin bitumen by 98.9 and 93.8 percent at the temperature of 64°C, respectively. Generally, J_{nr} values increased as the temperature rose to 82°C or the stress level changed to 3.2 kPa because bitumen acts like a viscous material. Noteworthily, this increment became greater at elevated stress and temperatures.

According to AASHTO M332, RMB is considered a sensitive bitumen to stress at all temperatures because J_{nrdiff} values exceed 75 %. Nonetheless, it extraordinarily resists permanent deformation based on the former findings (higher $R_{0.1}$ and $R_{3.2}$ and lower $J_{nr0.1}$, $J_{nr3.2}$) at all test temperatures and stress levels. Therefore, as other studies reported, a maximum value of 75 % for J_{nrdiff} may not be an appropriate limiting threshold for bitumen performance [29,30]. Overall, the increment of RMB's average percent of recovery and creep compliance indicates enhanced elastomeric properties and viscosity, leading to more resistance to rutting and, consequently, more durability of Rollpave. The aforementioned results are in line with the increased complex modulus at high temperatures, shown in Fig. 3.

5.3. Bitumen linear amplitude sweep test

After the PAV aging procedure, the fatigue characterizations of the virgin bitumen and RMB were assessed by conducting the LAS test. The stress-strain relationships of the samples at 20°C and 30°C are presented in Fig. 7. Comparatively, the virgin bitumen peaked at 8 % strain at 20°C, while RMB reached a peak point at 26.2 % strain at the same temperature. Also, due to the higher stiffness of the virgin bitumen, its peak stress is greater than the maximum stress of RMB. This means RMB behaved like an elastomer capable of being strained and stretched which can be justified by the presence of thermoplastic elastomer. In other words, incorporating thermoplastic elastomers can improve the flexibility of bitumen. This is due to their rubber-like properties and high extensibility, which allow them to undergo significant deformation without breaking or losing structural integrity. When added to bitumen, they enable the binder to stretch and accommodate movements, thereby enhancing its flexibility and supporting more deformations.

Regarding RMB performance at 30°C, higher strain levels are required for failure to occur when peak stress is the failure criterion in

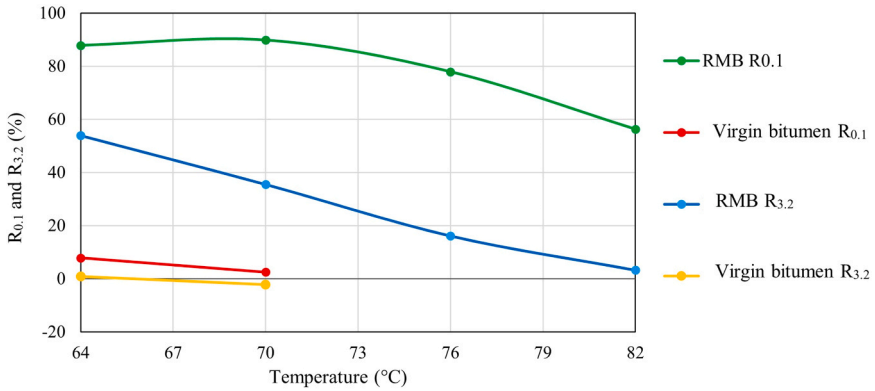

Fig. 6. $R_{0.1}$ and $R_{3.2}$ of RTFO-aged bitumen samples.

Table 6
Non-recoverable creep compliance indices of RTFO-aged bitumen samples.

Temperature	RMB			Virgin bitumen		
	$J_{nr0.1}$ (1/kPa)	$J_{nr3.2}$ (1/kPa)	J_{nrdiff} (%)	$J_{nr0.1}$ (1/kPa)	$J_{nr3.2}$ (1/kPa)	J_{nrdiff} (%)
64°C	0.032	0.213	555.04	2.827	3.43	21.34
70°C	0.046	0.723	1458.03	7.643	9.52	24.65
76°C	0.222	2.273	922.02	-	-	-
82°C	1.176	5.938	404.95	-	-	-

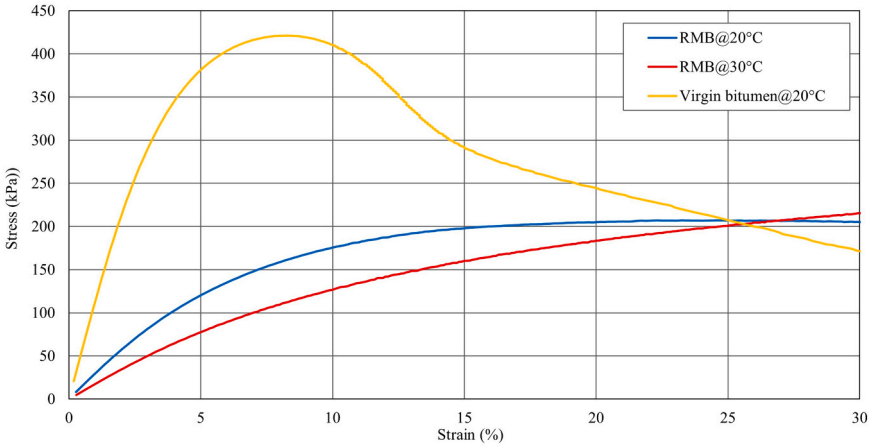

Fig. 7. Stress–strain relationships of bitumen samples at various temperatures.

the LAS test. In other words, RMB did not reach a stress peak point during the amplitude sweep. Therefore, the loading scheme of a continuous oscillatory strain sweep, which increases linearly to 30 %, as stated by AASHTO T101–14, may not be quite adequate for fatigue life evaluation of RMB. Thus, it is assumed that the maximum stress occurred at the strain of 30 % to calculate Nf.

The Damage Characteristic Curves (DCC) of PAV-aged bitumen samples are shown in Fig. 8. It exhibits a relationship between the integrity of the specimen (C) and intensified damage during the LAS test. It is shown that, unlike the virgin bitumen, the integrity of RMB declined gently at 20°C. For instance, a 70 % decrease in the integrity of virgin bitumen led to a damage intensity of 100, while a 50 % drop in the integrity of RMB caused the same damage, as demonstrated in Fig. 8(a) and (b). It can be concluded that since RMB has excellent stress relaxation ability, it exhibits remarkable damage endurance and durability. Expectantly, a rise in temperature caused an increment of damage endurance. More specifically, increasing the temperature to 30°C led to a 60 % growth of RMB integrity at the damage of 250. Plus, it lessened ultimate accumulated damage from 330 to 290, meaning that bitumen has more ability to endure damage.

As shown in Table 7, RMB has a higher D_f value and, consequently, a greater 'A' value, referring to better fatigue resistance performance. For example, Rollbit modification increased the 'A' value from 2.034E+06 to 2.033E+07 and reduced the absolute value of the 'B' by 13 percent at 20°C. As a result, at strain levels of 2.5 % and 5 %, the N_f values of RMB are 16 and 23 times greater than the corresponding values of the virgin bitumen, respectively. Additionally, the N_f values of RMB at both strain levels increased at 30°C, which aligns with logic since the bitumen is softer at high temperatures and has a better fatigue resistance [31]. It can be seen in Table 7 that the lower absolute value of the 'B' parameter not only increases fatigue life but also lessens the stress sensitivity of N_f.

5.4. *Asphalt four-point beam fatigue test*

Table 8 presents the flexural properties obtained from the four-point beam fatigue test conducted at 20°C for nearly 36,000 cycles. It includes the initial flexural stiffness measured at the 50_{th} load cycle, the final stiffness after 36,000 cycles, and the ratio between these values. As expected, higher initial stiffness and stiffness ratio were recorded at the low strain level test. Based on the average data, stiffness decreased by about 5 percent to 1448 MPa at the loading strain of 200 με while it reduced by almost 15 percent at 400 με. It can be concluded that the strain level highly influences the fatigue life under the strain-controlled mode.

Fig. 9(a) depicts the Rollpave stiffness versus loading cycles at 20°C and under 400 με loading for 600,000 cycles. It can be seen from the average values that the stiffness decreased rapidly in the early stage and then declined until it reached a plateau of about 1200 MPa. It then remained more or less stable in the following step. During the fatigue test, no cracks were detected in the Rollpave beam samples, indicating that the onset of fatigue cracks is delayed. In other words, the network formed between the ductile agent, thermoplastic elastomer, and bitumen particles enhances the endurance of asphalt and dissipates energy when subjected to forces. This energy dissipation helps reduce stress concentration and spreads fatigue damage across a broader area, preventing the formation of

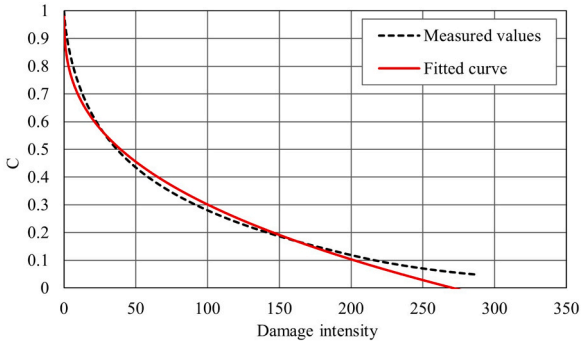

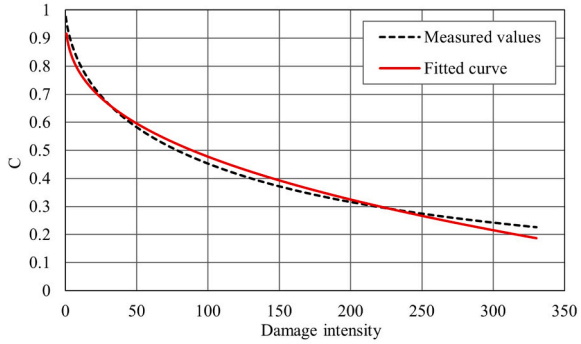

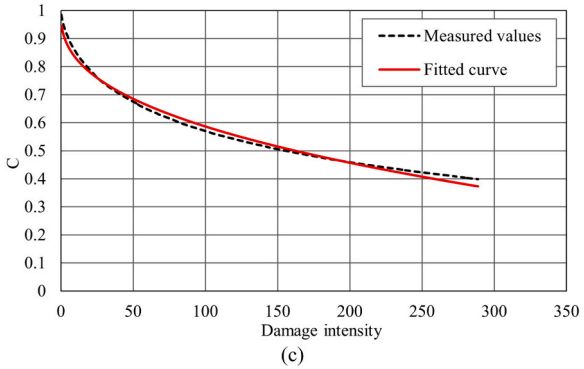

Fig. 8. Damage characteristic curves (DCC) of PAV-aged samples: (a) Virgin bitumen at 20°C, (b) RMB at 20°C, and (c) RMB at 30°C.

Table 7
Fatigue specifications of PAV-aged bitumen samples.

Temperature	RMB					Virgin bitumen				
	A	B	D_f	N_f (2.5 %strain)	N_f (5 %strain)	A	B	D_f	N_f (2.5 %strain)	N_f (5 %strain)
20°C	2.033×10^7	-3.55	214	786,218	67,127	2.034×10^6	-4.06	55	49,108	2936
30°C	1.981×10^7	-3.29	260	972,183	99,419	-	-	-	-	-

cracks and fractures. Additionally, thermoplastic elastomers generally improve the cohesion and adhesion properties of bitumen and asphalt mixtures. These improvements in bonding strength contribute to the overall resistance of the asphalt against distress. Moreover, the average phase angle value is nearly constant and fluctuates between 29 and 32 degrees, as shown in Fig. 9(b). This implies that the internal structure of Rollpave not only resists breaking but also maintains a consistent viscoelastic characteristic under fatigue loading.

To better understand the performance of Rollpave, the initial stiffness of Rollpave is compared with the initial stiffness values of

Table 8
Flexural properties of Rollpave from four-point fatigue test at 20°C.

Strain level (με)	Loading cycles	Sample Number	Initial flexural stiffness (MPa)	Average initial stiffness (MPa)	Flexural stiffness (MPa)	Average stiffness (MPa)	Stiffness ratio (%)
200	36,200	1	1424		1364		95.79
200	36,200	2	1453	1522	1354	1448	93.20
200	36,200	3	1687		1626		96.38
400	36,200	1	1499		1266		84.46
400	36,200	2	1408	1466	1196	1240	84.94
400	36,200	3	1491		1258		84.37

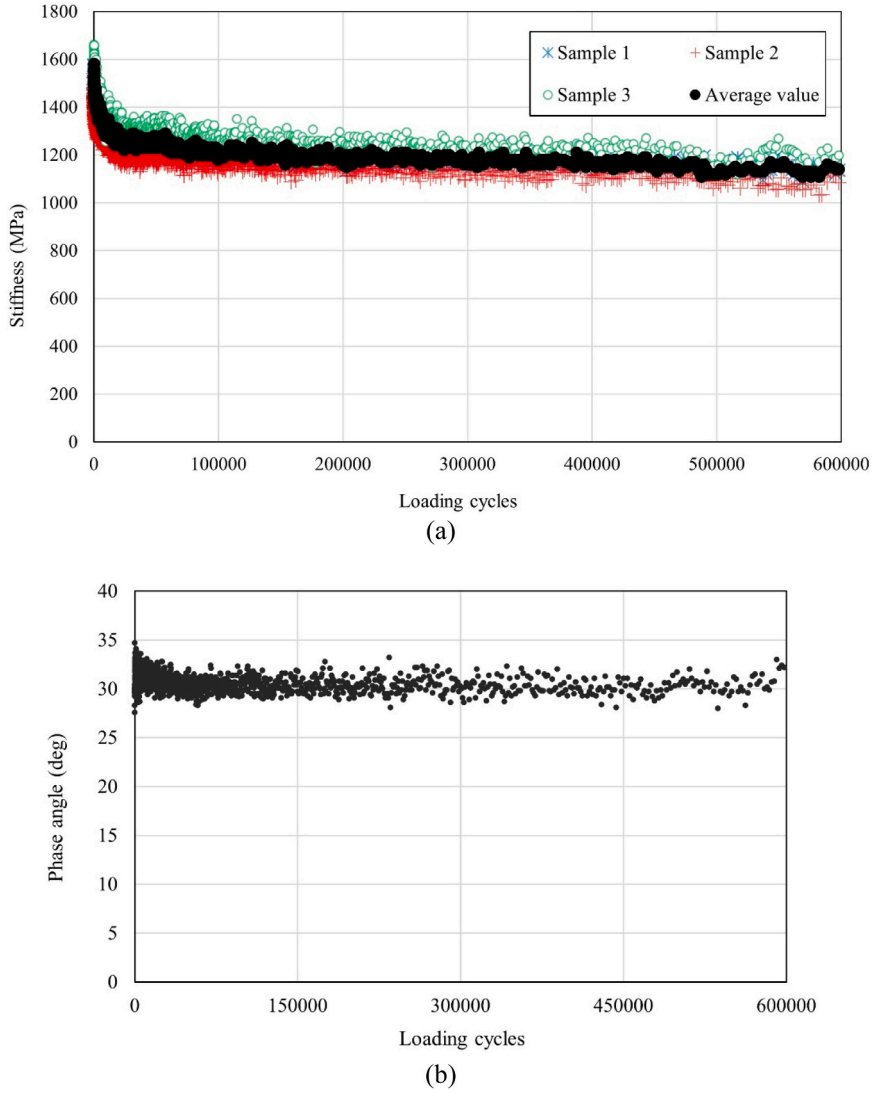

Fig. 9. (a) Flexural stiffness and (b) phase angle VS loading cycles for Rollpave at 20°C and under 400με loading.

different modified asphalt in previous studies. as outlined in Table 9. It shows that the initial stiffness of samples named VG10 and VG30 exceeds the initial stiffness of Rollpave by about four times and nine times, respectively, under both strain levels of 200 με or 400 με [32]. Moreover, it shows that the corresponding value of the neat mixture and SBS-modified mixture measured by Cheng et al. is about 7500 MPa and 4500 MPa greater than Rollpave's under the strain of 400 με, respectively [33]. This comparison indicates that Rollpave behaves softer and has better deformation ability, resulting in superior fatigue resistance.

Generally, the number of load cycles required to reach a 50 % reduction in initial stiffness is considered as a termination for evaluating fatigue performance. However, considering the applied strain level and loading cycles, the samples maintained their

Table 9
The initial flexural stiffness of Rollpave and other asphalt mixtures.

Mixture type	Description	Temperature (°C)	Strain level (με)	Initial flexural stiffness (MPa)	Reference
Rollpave	-	20	200	1522	This study
Rollpave	-	20	400	1466	
VG10	Penetration at 25 °C (0.1 mm):104	20	200	7200	[32]
			400	6800	
VG30	Penetration at 25 °C (0.1 mm): 45	20	200	14,000	
			400	13,500	
Neat mixture	-	20	400	10,000	[33]
SBS-modified mixture	-	20	400	6000	

stiffness without experiencing a 50 % loss. Consequently, the approach involving a one-stage Weibull Survivor Function, as shown in Eq. 11, was employed on the average values to extrapolate the outcome until the point of failure [24,25,34,35]. In addition, a damage model introduced and verified by Zou et al. was applied to calculate the fatigue damage of Rollpave [35]. Eq. 12 illustrates the generated model of fatigue damage degree.

$$Ln(-Ln(SR)) = \gamma.Ln(N) + Ln(\lambda) \tag{11}$$

$$D = 1 - \exp\left(-\lambda'\left(\frac{N}{N_f}\right)^{\gamma'}\right) \tag{12}$$

Where:

SR is the stiffness ratio, asphalt stiffness at cycle i divided by initial asphalt stiffness. And, N is the number of cycles. Also, γ is the slope of the linear regression of the Ln(-Ln(SR)) versus Ln(N). Ln(λ) is the intercept of the linear regression of the Ln(-Ln(SR)) versus Ln (N). Additionally, D and N_f are the degree of damage and the number of load cycles at the point of fatigue failure, respectivly. λ' and γ' are the fitting parameters.

Fig. 10 (a) presents Ln(-Ln(SR)) versus Ln(N) and a fitted line with the linear part of the average data. Also, the curve of fatigue damage degree with loading cycles is demonstrated in Fig. 10 (b). At first, Eq. 11 was solved for cycles to failure by setting the SR value at 0.5, and then Eq. 12 was solved by utilizing the predicted value of N_f to calculate the D parameter. Table 10 encompasses the parameters of the equations above and the predicted values for Rollpave. The extraordinary fatigue life of Rollpave can be justified by the combination of elastomers and ductile agents, which have rubbery behaviors. Furthermore, incorporating bio-oil compounding agent might have contributed to enhancing the flexibility of Rollpave, and the inclusion of EPDM in RMB has a positive impact on fatigue life [36,37]. It should be noted that the optimal RMB content for Rollpave in this study is 7.5 % of the aggregate weight, which plays a substantial role in fatigue life, and this high amount of bitumen leads to a longer fatigue life for the asphalt. According to above-mentioned results, it can be said that Rollpave demonstrates appropriate performance against fatigue cracking.

5.5. Dynamic creep test

Fig. 11 depicts the cumulative permanent strain of specimens at temperatures of 50°C and 60°C under 400 kPa dynamic creep loading. Generally, the creep curve is divided into three stages, as reported by previous studies [28,38]. The primary stage illustrates recoverable elastic strain, the secondary stage demonstrates viscoelastic strain, and the third stage presents irrecoverable plastic strain.

Vital differences can be seen among the creep curves in Fig. 11. While Rollpave at 50°C did not go through the secondary stage, all permanent stages can be seen in the creep curve at 60°C. Additionally, the average data reveals that Rollpave entered the third stage after approximately 3400_{th} loading cycles at 60°C and reached nearly 30,000 με around the 5000_{th} loading cycle, while the cumulative permanent strain at 50°C was well below 20,000 με in the 9000_{th} loading cycle. This sharp growth in permanent deformation with an increasing 10 degrees in temperature can be justified by the MSCR test results, indicating that the creep performance of RMB is susceptible to temperature. Accordingly, the significance of temperature becomes evident in the permanent deformation behavior of Rollpave, as both the total permanent strain and the rate of increment increase at higher temperatures.

This behavior may be attributed to the structure of RMB at elevated temperatures, as the thermoplastic elastomer network could potentially break, allowing the characteristics of bio-oil to dominate in the bitumen and make it temperature-sensitive and softer. As a result, Rollpave is prone to permanent creep deformation at high temperatures. Also, it can be added that the first stage represents recoverable elasticity, and the second stage represents the viscoelastic behavior of the mixture. Therefore, due to the increase in viscosity caused by temperature growth to 60°C, Rollpave underwent more permanent deformation. On the other hand, the same reasoning holds true for the lower temperature (50°C in this study), which has caused the second phase not to form and permanent strain to accumulate at a lower rate.

Due to the lack of a control sample, the average creep performance of Rollpave is compared with the permanent strain of asphalt from previous studies, as shown in Table 11. The results provide valuable insights into the better creep performance of Rollpave compared to other asphalt mixtures under various temperatures and stress conditions. More explicitly, Rollpave withstands 9000 loading cycles before reaching the strain of 19,000 με at 50°C, while modified SMA with crumb rubber and trans-polyoctenamer exhibits a higher permanent strain through 1800 loading cycles. Furthermore, the Flow Number (FN) of Rollpave at 60°C was compared with the corresponding values of modified asphalts reported by Pouranian MR et al. [39]. Table 12 demonstrates that FN of

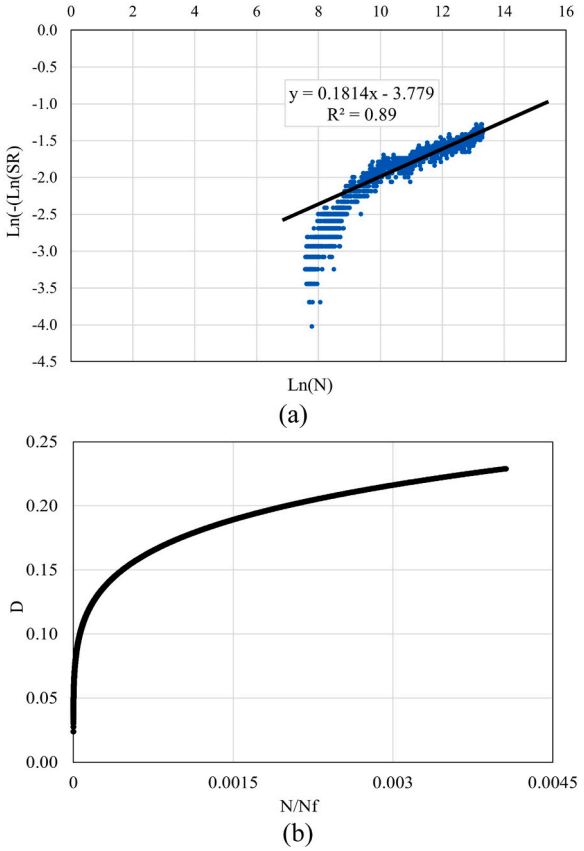

Fig. 10. (a) Ln(-Ln(SR)) versus Ln(N) and (b) damage degree curves with loading cycles for Rollpave at 20°C and under 400με loading.

Table 10
Parameters for Eqs. 2 and 3 as well as Df and D for Rollpave at 20°C and under 400με loading.

Asphalt Type	γ	Ln(λ)	Ln(N)	λ'	γ'	D (At N_f)
Rollpave	0.1814	-3.779	18.8	0.854	0.216	0.57

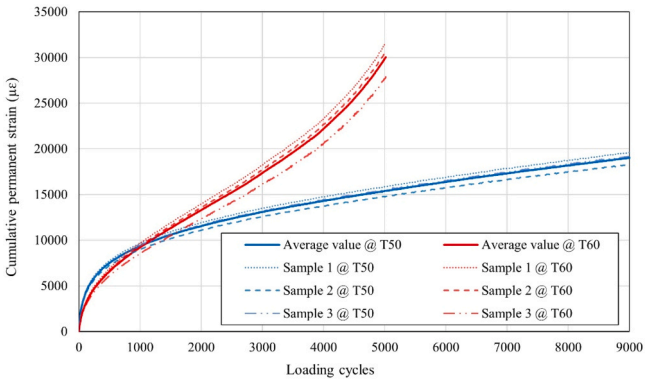

Fig. 11. Creep curve for Rollpave at 50°C and 60°C under 400 kPa stress level.

Rollpave is significantly more than the corresponding values of Ethylene-Vinyl-Acetate (EVA) and SBS-modified mixtures. In general, it can be stated that Rollpave has good resistance to permanent creep deformation at high operating temperatures.

Finally, the creep performance of the Rollpave mixture was modeled by Zhou's three-stage model. This model used a power law

Table 11
The cumulative permanent strain of Rollpave and other asphalt mixtures.

Mixture type	Description	Temperature (°C)	Stress (kPa)	Loading cycles	permanent strain (με)	Reference
Rollpave	-	50	400	9000	19,000	This study
Rollpave	-	60	400	5000	30,000	
Control	SMA	50	400	1500	100,000	[40]
12 R	SMA modified with 12 % crumb rubber	50	400	1800	45,000	
12 R 4.5 V	12 % crumb rubber + 4.5 % trans-polyoctenamer	50	400	1800	39,000	
Control	SMA	40	200	1150	70,000	[41]
POC-00	SMA modified with 50 % Palm oil fuel ash	40	200	1700	70,000	
POC-60	SMA modified with 50 % Palm oil fuel ash and 60 % Palm oil clinker	40	200	1800	32,000	
Control	Hot Mix Asphalt (HMA)	50	210	1400	30,000	[42]
0.18 % fibre	HMA modified with 0.18 % Polyolefin-glass fibre	50	210	2700	25,000	
Control	HMA	40	400	1000	10,000	[43]
1 % PET	HMA modified with 5 % Polyethylene Terephthalate	40	400	2900	10,000	

Table 12
FN values of Rollpave, EVA-modified, and SBS-modified mixtures.

Temperature (°C)	Stress (kPa)	Rollpave	EVA-modified	SBS-modified
60	350	N/A	300	583
	400	3400	N/A	N/A
	450	N/A	160	183

function, a linear function, and an exponential function for stages one to three, as shown below. The findings are displayed in Table 13.

$$\text{Primary stage}: \varepsilon_p = aN^b, \quad N \le N_{PS} \tag{13}$$

$$\text{Secondary stage}: \varepsilon_p = \varepsilon_{PS} + c(N - N_{PS}), \quad \varepsilon_{PS} = aN_{PS}{}^b, \quad N_{PS} \le N \le N_{ST} \tag{14}$$

$$\text{Tertiary stage}: \varepsilon_p = \varepsilon_{ST} + d\left(e^{f(N-N_{ST})} - 1\right), \quad \varepsilon_{ST} = \varepsilon_{PS} + \quad c(N_{ST} - N_{PS}), \quad N \ge N_{ST} \tag{15}$$

Where:

ε_p is the accumulated permanent strain and N is the number of load repetitions. N_{PS} and N_{ST} are the load repetitions corresponding to the secondary and tertiary stage initiation. ε_{PS} and ε_{ST} are the permanent strains corresponding to the secondary and tertiary stage initiation; also, a, b, c, d, and f are the material constants.

6. Conclusions

Recent efforts to develop a pavement preservation approach that is both efficient and superior in quality have yielded Rollpave, a prefabricated, easily deployable, and thin layer capable of being unfurled akin to a carpet atop existing pavements, consequentially streamlining and ameliorating construction or maintenance durations. Within this study, the resilience of Rollpave was evaluated, encompassing its propensity for creep and fatigue. To evaluate the creep performance, the BBR, MSCR, and dynamic creep tests were conducted. Also, to explore the fatigue performance of Rollpave, investigations were conducted through LAS and four-point beam fatigue tests. The ensuing outcomes are outlined below:

- BBR test results highlight the decreased creep stiffness and the higher m-value of RMB compared to the original bitumen. RMB's creep stiffness at −12°C is about half of the virgin bitumen. Additionally, despite a 6-degree drop in temperature to −18°C, the RMB creep stiffness is still less than the creep stiffness of virgin bitumen at −12°C.

Table 13
Creep curve models based on Zhou's model.

Temperature (°C)	First stage		Second stage		Third stage
	Model	End of the stage	Model	End of the stage (FN)	Model
50	ε_p=1024.2×N$^{0.318}$	N/A	N/A	N/A	N/A
60	ε_p=316.2×N$^{0.488}$	N=1296	ε_p=10,464.585+4.023 (N-1296)	N=3400	ε_p=18,930.246 + 12,084.825(e$^{(0.00,039,784 (N-3400))}$ −1)

- MSCR test results demonstrate RMB has an outstanding resistance against creep deformation, considering increased values of $R_{0.1}$ and $R_{3.2}$ and decreased values of $J_{nr0.1}$ and $J_{nr3.2}$ across all testing temperatures compared to virgin bitumen. However, MSCR and asphalt dynamic creep test shows that although Rollpave is resistant to permanent creep deformation at high operating temperatures, it is sensitive to stress and temperature. Rollpave entered the third stage after approximately 3400_{th} loading cycles at 60°C and reached nearly 30,000 με around the 5000_{th} loading cycle, while the cumulative permanent strain at 50°C was well below 20,000 με in the 9000_{th} loading cycle.
- Considering the results from the LAS test, RMB demonstrates elastomeric characteristics with excellent flexibility and stretchability leading to greater fatigue resistance compared to virgin bitumen, as evidenced by the elevated 'A' values and the lower absolute 'B' values. Consequently, the Nf values of RMB exhibited a significant increase at both strain levels of 2.5 % and 5 %. The results of the four-point beam fatigue test show that the sample retained its stiffness without encountering a 50 % loss even after loading cycles and no cracks were detected in the Rollpave beam during the test. This implies that the internal structure of Rollpave not only resists breaking but also maintains a consistent viscoelastic characteristic under fatigue loading.
- Overall, the authors believe that the enhanced fatigue life of Rollpave can be attributed to the combination of modifiers, which might form an elastomeric network enriching asphalt fatigue resistance. It is important to note that the optimal RMB content of Rollpave is 7.5 % of the aggregate weight, which has a significant impact on the fatigue life.

CRediT authorship contribution statement

Sayyed Mahdi Abtahi: Writing – review & editing, Supervision, Project administration, Funding acquisition, Conceptualization. **Mahdi Shojaei:** Writing – original draft, Visualization, Resources, Methodology, Investigation, Formal analysis. **Hajar Share Isfahani:** Writing – review & editing, Supervision, Funding acquisition, Conceptualization.

Declaration of Competing Interest

The authors declare that they have no known competing financial interests or personal relationships that could have appeared to influence the work reported in this paper

Data availability

No data was used for the research described in the article.

References

[1] J. Wang, et al., Laboratory and field performance evaluation of high-workability ultra-thin asphalt overlays, Materials 15 (6) (2022) 2123.
[2] Y. Dong, et al., Study on road performance of prefabricated rollable asphalt mixture, Road. Mater. Pavement Des. 18 (sup3) (2017) 65–75.
[3] Erkens, S. *et al.*, 2015. On the need for innovation in road engineering A Dutch example. in: Proceedings of the Thirrd International Symposium on Asphalt Pavements and Environment, Sun City, South Africa.
[4] R. Naus, et al., Rollpave, a prefabricated asphalt wearing course, in: Proceedings ISAP Nagoya (Preprint) (2010).
[5] A. Tezel, L. Koskela, Off-site construction in highways projects: management, technical, and technology perspectives from the United Kingdom, Constr. Manag. Econ. 41 (6) (2023) 475–499.
[6] S. Ling, et al., A comprehensive review of tire-pavement noise: generation mechanism, measurement methods, and quiet asphalt pavement, J. Clean. Prod. 287 (2021) 125056.
[7] Z. Ye, et al., Optimization of embedded sensor packaging used in rollpave pavement based on test and simulation, Materials 15 (6) (2022) 2283.
[8] Q. Tan, H. Zhu, H. Zhao, et al., Innovative treatment of crack defects and skid resistant deficiencies in old asphalt pavement using a prefabricated flexible ultrathin overlay, J. Mater. Civ. Eng. 36 (5) (2024) 4024053.
[9] Y. Dong, et al., Self-healing performance of rollable asphalt mixture, J. Mater. Civ. Eng. 31 (7) (2019) 4019117.
[10] Hofman, R. and van Vliet, W., 2011. Results Dutch PERS test on A50. in: Proceedings of the INTER-NOISE and NOISE-CON Congress and Conference Proceedings, Institute of Noise Control Engineering, 3396–3404.
[11] Ingram, L.S. *et al.*, 2004. Superior Materials, Advanced Test Methods, and Specifications in Europe, United States. Federal Highway Administration.
[12] D. Wang, et al., Feasibility study on the innovative construction method of a prefabricated and rollable road, Bautechnik 90 (10) (2013) 614–621.
[13] D.A.I. Shuning, et al., Study on the influence of basalt fiber content on the road performance of rollable pavement, New Build. Mater. /Xinxing Jianzhu Cailiao 46 (4) (2019).
[14] J. Yang, et al., Prefabricated flexible conductive composite overlay for active deicing and snow melting, J. Mater. Civ. Eng. 30 (11) (2018) 04018283.
[15] Q. Tan, H. Zhu, S. Yang, et al., Precast assembled road paving technology: progress and prospects, Materials (2024).
[16] Y.S. Dong, et al., Research of influencing factor on the bending property of asphalt mixture based on grey correlation entropy. in: Applied Mechanics and Materials, Trans Tech Publ, 2013, pp. 1923–1927.
[17] Houben, L.J.M. *et al.*, 2004. APT testing of modular pavement structure 'Rollpave'and comparison with conventional asphalt motorway structures. in: Proceedings of the the Second International Conference on Accelerated Pavement Testing, Minneapolis, USA. Citeseer.
[18] R. Jing, et al., Rheological, fatigue and relaxation properties of aged bitumen, Int. J. Pavement Eng. 21 (8) (2020) 1024–1033.
[19] B. Budziński, et al., Influence of bitumen grade and air voids on low-temperature cracking of asphalt, Case Stud. Constr. Mater. 19 (2023) e02255.
[20] H.U. Bahia, et al., The bending beam rheometer; a simple device for measuring low-temperature rheology of asphalt binders (with discussion), J. Assoc. Asph. Paving Technol. 61 (1992).
[21] L. Porot, et al., Multiple stress creep recovery test to differentiate polymer modified bitumen at high temperature, J. Test. Eval. 51 (4) (2023) 2168–2178.
[22] Y. Kim, et al., A simple testing method to evaluate fatigue fracture and damage performance of asphalt mixtures (with discussion), J. Assoc. Asph. Paving Technol. 75 (2006).
[23] T. Su, et al., Premature pavement distresses of cracks and rutting analysis and mechanical analysis in ultra-thin asphalt pavement, *Pavement Mater., Struct., Perform.* (2014) 167–178.
[24] Tsai, B.-W., 2001. High-temperature Fatigue and Fatigue Damage Process of Aggregate-asphalt Mixes, University of California, Berkeley.
[25] B.-W. Tsai, et al., Application of Weibull theory in prediction of asphalt concrete fatigue performance, Transp. Res. Rec. 1832 (1) (2003) 121–130.

[26] A. Khodaii, A. Mehrara, Evaluation of permanent deformation of unmodified and SBS modified asphalt mixtures using dynamic creep test, Constr. Build. Mater. 23 (7) (2009) 2586–2592.
[27] T.B. Moghaddam, et al., Experimental characterization of rutting performance of polyethylene terephthalate modified asphalt mixtures under static and dynamic loads, Constr. Build. Mater. 65 (2014) 487–494.
[28] F. Zhou, et al., Verification and modeling of three-stage permanent deformation behavior of asphalt mixes, J. Transp. Eng. 130 (4) (2004) 486–494.
[29] A. Behnood, et al., High temperature properties of asphalt binders: statistical and experimental comparison of MSCR and PG grading systems, Transp. Res. Rec. J. Transp. Res. Board 2574 (2016) 131–143.
[30] S. Hassanpour-Kasanagh, et al., Rheological properties of asphalt binders modified with recycled materials: a comparison with Styrene-Butadiene-Styrene (SBS), Constr. Build. Mater. 230 (2020) 117047.
[31] F. Safaei, C. Castorena, Temperature effects of linear amplitude sweep testing and analysis, Transp. Res. Rec. 2574 (1) (2016) 92–100.
[32] M. Chauhan, A. Narayan, Effect of moisture on fatigue characteristics of asphalt concrete mixtures. in: Proceedings of the Fifth International Symposium on Asphalt Pavements & Environment (APE) 5, Springer, 2020, pp. 356–366.
[33] H. Cheng, et al., Fatigue behaviours of asphalt mixture at different temperatures in four-point bending and indirect tensile fatigue tests, Constr. Build. Mater. 273 (2021) 121675.
[34] M. Zaumanis, et al., Influence of six rejuvenators on the performance properties of Reclaimed Asphalt Pavement (RAP) binder and 100% recycled asphalt mixtures, Constr. Build. Mater. 71 (2014) 538–550.
[35] X. Zou, et al., Damage analysis four-point bending fatigue tests on stone matrix asphalt using dissipated energy approaches, Int. J. Fatigue 133 (2020) 105453.
[36] A. Chegenizadeh, et al., Ethylene propylene diene monomer (EPDM) effect on asphalt performance, Buildings 11 (8) (2021) 315.
[37] X. Yang, et al., Mechanical performance of asphalt mixtures modified by bio-oils derived from waste wood resources, Constr. Build. Mater. 51 (2014) 424–431.
[38] Witczak, M.W., 2002. Performance Evaluation of Arizona Asphalt Rubber Mixtures Using Advanced Dynamic Material Characterization Tests.
[39] M.R. Pouranian, et al., The effect of temperature and stress level on the rutting performance of modified stone matrix asphalt, Road. Mater. Pavement Des. 21 (5) (2020) 1386–1398.
[40] H.Y. Katman, et al., Evaluation of permanent deformation of unmodified and rubber-reinforced SMA asphalt mixtures using dynamic creep test, Adv. Mater. Sci. Eng. 2015 (2015).
[41] A.M. Babalghaith, et al., Performance evaluation of stone mastic asphalt (SMA) mixtures with palm oil clinker (POC) as fine aggregate replacement, Constr. Build. Mater. 262 (2020) 120546.
[42] H. Ziari, A. Moniri, Laboratory evaluation of the effect of synthetic Polyolefin-glass fibers on performance properties of hot mix asphalt, Constr. Build. Mater. 213 (2019) 459–468.
[43] T.B. Moghaddam, et al., Evaluation of permanent deformation characteristics of unmodified and Polyethylene Terephthalate modified asphalt mixtures using dynamic creep test, Mater. Des. 53 (2014) 317–324.